Journal of Biomechanics 46 (2013) 1242–1247

Contents lists available at SciVerse ScienceDirect

Journal of Biomechanics

journal homepage: www.elsevier.com/locate/jbiomech
www.JBiomech.com

Counter-effect of constrained dynamic loading on osteoporosis in ovariectomized mice

Hao Li, Rui-Xin Li, Zong-Ming Wan, Cheng Xu, Jian-Yu Li, Qing-Xin Hao, Yong Guo, Lu Liu, Xi-Zheng Zhang *

Institute of Medical Equipment, Academy of Military Medical Sciences, Tianjin 300161, China

A R T I C L E I N F O

Article history:
Accepted 27 February 2013

Keywords:
Osteoporosis
Dynamic loading
Counter-effect
Osteogenesis
Mechanical properties

A B S T R A C T

In recent years, dynamic mechanical loading has been shown to effectively enhance bone remodeling. The current study attempted to research the counter-effect of constrained dynamic loading on osteoporosis (OP) in ovariectomized (OVX) mice. Female Kunming (KM) mice were randomly divided into 2 groups: SHAM and OVX. The right ulnas of the OVX mice were subjected to a 4-week constrained dynamic loading protocol, and the mechanical properties, trabecular micromorphology parameters and biochemical indices of osteogenesis were evaluated. We detected higher levels of tissue alkaline phosphatase (AKP) and serum bone gamma-carboxyglutamic-acid-containing proteins (BGPs), better trabecular micromorphology parameters and ulnar mechanical properties in the loading group than in the nonloading group. In summary, constrained dynamic loading could prevent ovariectomy-induced osteoporosis by facilitating osteogenesis, improving trabecular microstructure and enhancing bone mechanical properties.

1. Introduction

Bones are mechanically sensitive tissues that operate throughout their life span in dynamic stress/strain conditions that require "balance" between structural, functional and mechanical properties. It is generally believed that the "mechanostat" acts as the mediator between mechanical stimulation and the bone biologic response and there accordingly should be thresholds of mechanical use, such as typical peak strain, that help determine where and how the bone (re)models (Frost, 1991, 1997).

Postmenopausal women worldwide suffer most from osteoporosis, which is typically characterized by a lower bone density and a higher fracture risk (Karlsson et al., 2005; Marcus and Majumdar, 2001). Fortunately, increasing evidence suggests that loading forms, such as amplitude, frequency and intervals, play important roles in mechanics-induced bone remodeling. Broadly speaking, under the same or similar levels of strain distribution, the osteogenic capacity of bone weakens from dynamic loading to static loading, compression to tension, and loading with intervals to no intervals. Mechanical loading with a constrained amplitude and frequency (particularly 15–30 Hz) could cause obvious osteogenesis and improve the histomorphology and mechanical behavior of cancellous bone (Kaspar et al., 2002; Lanyon, 1996; Robling et al., 2002; Skerry, 1997).

In the present study, we hypothesized that dynamic loading producing 200 –3000 $\mu\varepsilon$ of local peak strain in bone would be beneficial for bone formation based on the "mechanostat" theory (Frost, 1987a, 1987b). We built a 3D model of the mouse ulna using micro-CT, determined the loading conditions using a finite element analysis (FEA) to control the distribution of strain in the ulna and chose classical indices of osteogenesis and mechanical properties, including tissue AKP, serum BGP, trabecular microstructure parameters, fracture displacement, fracture stress and fracture energy (Brown et al., 1987; Ito et al., 2002; Nian et al., 2009; Pauchard et al., 2008; Zhao et al., 2011), to detect bone formation.

The aim of this study was to evaluate the counter-effect of constrained dynamic loading during estrogen deficiency-induced OP formation using the mouse ovariectomy model of OP (Kalu, 1991; Peng et al., 1997; Rodgers et al., 1993).

2. Materials and methods

2.1. Animals and materials

Female KM mice were purchased from the laboratory animal center of the Academy of Military Medical Sciences in Beijing. The Bicinchoninic Acid (BCA) Protein Assay Kit, Mouse OT/BGP ELISA Kit and AKP Assay Kit were obtained from the Nanjing Jiancheng Bioengineering Institute.

* Corresponding author. Tel.: +86 02284656716.
E-mail address: z84656716@yahoo.com (X.-Z. Zhang).

0021-9290/$ - see front matter © 2013 Elsevier Ltd. All rights reserved.
http://dx.doi.org/10.1016/j.jbiomech.2013.02.016

2.2. Experimental design

A total of 21 female 2-month-old KM mice were randomly divided into 2 groups: SHAM (7 mice) and OVX (14 mice). The mice in the former group were sham operated, while the latter were ovariectomized. Thereafter, the right ulnas of all the OVX mice were subjected to constrained dynamic loading (with a diaphyseal peak strain 1000 –3000 $\mu\varepsilon$ and a frequency of 15 Hz) for 15 min every 3rd day over a period of 4 weeks. Finally, the ulnas were harvested and divided into 3 groups, SHAM (ulnas from the SHAM group), OVX+Loading (right ulnas from the OVX group) and OVX (left ulnas from the OVX group), and their mechanical properties, micromorphology parameters, tissue AKP and serum BGP content were analyzed.

2.3. Identification of the constrained dynamic loading parameters

Using FEA, loading parameters were identified that could avoid operational influences during classical strain measurement (strain gauge) in vivo. A 3D model of the mouse ulna obtained by micro-CT (SkyScan 1076, Belgium) was imported into ANSYS 12.0 and free meshed. Material properties were simplified to be isotropic and have linear elasticity under infinitesimal conditions, and we chose the modulus of cortical bone (E_1=18.1 GPa, ν_1=0.3) and cancellous bone (E_2=0.4 GPa, ν_2=0.3) (Brennan et al., 2011; Cory et al., 2010; Homminga et al., 2002; Ito et al., 2002; Pauchard et al., 2008; Zhang et al.,. 2008) as limiting boundaries. Increasing compressive displacement and static loads were applied along the axial direction to calculate the diaphyseal average von Mises strain, according to which we drew the *integral strain–diaphyseal strain* curve and the *load–diaphyseal strain* curve. Using curve-fitting, we took into account the attenuation effect when loading in vivo and determined the static preload and the amplitude of dynamic loading. A final verification of the strain distribution statistics by FEA was also performed.

2.4. Tests of ulnar osteogenic activity and mechanical behavior

Tissue AKP was tested using a BCA Protein Assay Kit and an AKP Assay Kit. Serum BGP was tested using a Mouse OT/BGP ELISA Kit. Micromorphology parameters of ulnar cancellous bone, including percent trabecular area (B.Ar/T.Ar), trabecular pattern factor (Tb.Pf), trabecular thickness (Tb.Th), trabecular separation (Tb.Sp) and trabecular number (Tb.N), were analyzed by the post-processing of micro-CT images. The mechanical properties of the ulna were determined by the classical three-point bending test on an INSTRON 5865 (Instron Corporation, America) with the following parameters: 10 mm gauge length, 0.5 N preload and 3 mm/min loading rate, outputting fracture displacement/strain, fracture stress and fracture energy.

2.5. Statistical analysis

All data were presented as the mean ± S.D. from at least three independent experiments. Significant differences were evaluated by a one-way analysis of variance (ANOVA) followed by the least significant difference (LSD)-*t* test. Significance was defined at $p<0.05$.

3. Results

A 3D model of the mouse ulna was free meshed with element-type Solid 92, 18,064 elements and 27,971 nodes in ANSYS 12.0. The *integral strain–diaphyseal strain curve* and the *load–diaphyseal strain curve* under limiting material constants (E_1=18.1 GPa, E_2=0.4 GPa, $\nu_1=\nu_2$=0.3) are shown in Figs. 1 and 2.

Using curve-fitting and theoretical calculations, we finally selected dynamic loading conditions as the sinusoidal displacement curve ($y=0.045\ \sin(30\pi\times t)$ (mm)) starting from an equilibrium position with a 0.5 N static preload because, under this condition, the 0.5 N preload and sinusoidal displacement with an amplitude of 0.045 mm will cause 220 $\mu\varepsilon$ and 3000 $\mu\varepsilon$ diaphyseal peak strain in the ulna, respectively. Fig. 3 shows the ideal and actual loading modes. In Fig. 4, we are clear of the strain distribution in the ulna at a glance. Considering the inevitable absorption of impact energy by the joints and muscle, the actual total diaphyseal peak strain should be less than 3220 $\mu\varepsilon$ and is more likely to be 1000–3000 $\mu\varepsilon$, which is our favored scenario.

Vaginal smears in the first 5 postoperative days are shown in Fig. 5. Mice in the SHAM group had a normal life with a regular estrous cycle (Fig. 5(b)), while mice in the OVX group experienced dioestrum (Fig. 5(c)), suggesting that the ovariectomy was successful.

The HE-stained, non-decalcified slices in Fig. 6 qualitatively show the changes in the trabecular bone in each group after the 4-week dynamic loading procedure.

The changes in the micromorphology parameters of cancellous bone were in accordance with the qualitative observations, as shown in Fig. 7. We defined the proximal and distal ends of the ulna and chose the sections of cancellous bone 3 mm from the proximal end and 1.5 mm from the distal end as our regions of interest, as shown in Fig. 7(a). The scanning parameters were set at a 50 kV voltage and 9 μm slices. The micromorphology parameters were calculated and are presented as histograms with statistical significance in Fig. 7(b) and (c). We found that the trabecular bone in the OVX group deteriorated with a smaller B.Ar/T.Ar, thinner Tb.Th, larger Tb.Sp and more Tb.N when compared with the SHAM group, while the microstructure of the trabecular bone in the OVX+Loading group improved with a higher B.Ar/T.Ar, thicker Tb.Th and smaller Tb.Sp when compared with the OVX group.

We evaluated the mechanical properties of the ulna using a three-point bending test on an INSTRON 5865, and the mechanical

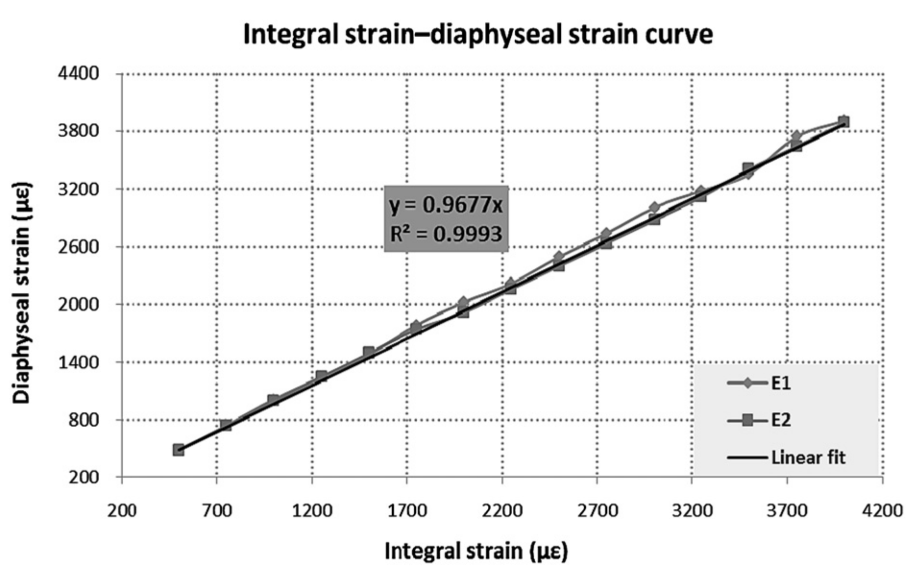

Fig. 1. Integral strain–diaphyseal strain curve and linear fit of the ulna.